Bioresource Technology 317 (2020) 123984

Contents lists available at ScienceDirect

Bioresource Technology

journal homepage: www.elsevier.com/locate/biortech

A novel carboxylesterase from *Acinetobacter* sp. JNU9335 for efficient biosynthesis of Edoxaban precursor with high substrate to catalyst ratio

Zhe Dou, Guochao Xu, Ye Ni*

Key Laboratory of Industrial Biotechnology, Ministry of Education, School of Biotechnology, Jiangnan University, Wuxi 214122, PR China

GRAPHICAL ABSTRACT

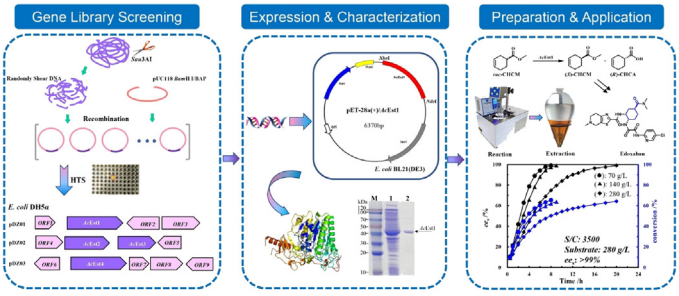

ARTICLE INFO

Keywords:
Carboxylesterase
High-throughput screening
Genome shotgun library, kinetic resolution
Methyl 3-cyclohexene-1-carboxylate
Substrate to catalyst ratio

ABSTRACT

A novel carboxylesterase *Ac*Est1 was identified from *Acinetobacter* sp. JNU9335 with high efficiency in the biosynthesis of chiral precursor of Edoxaban through kinetic resolution of methyl 3-cyclohexene-1-carboxylate (CHCM). Sequence analysis revealed *Ac*Est1 belongs to family IV of esterolytic enzymes and exhibits < 40% identities with known carboxylesterases. The optimum pH and temperature of recombinant *Ac*Est1 are 8.0 and 40 °C. Substrate spectrum analysis indicated that *Ac*Est1 prefers substrates with short acyl and alcohol groups. *Ac*Est1 was highly active in the hydrolysis of CHCM with k_{cat} of 1153 s^{-1} and displayed high substrate tolerance. As much as 2.0 M (280 $g{\cdot}L^{-1}$) CHCM could be enantioselectively hydrolyzed into (*S*)-CHCM by merely 0.08 $g{\cdot}L^{-1}$ *Ac*Est1 with ee_s of > 99% (*S*) and substrate to catalyst ratio (S/C) of 3500 $g{\cdot}g^{-1}$. These results indicate that the novel *Ac*Est1 is a promising biocatalyst in the synthesis of chiral carboxylic acids.

1. Introduction

Optically active 3-cyclohexene-1-carboxylic acid (CHCA) is an important chiral carboxylic acid with a special unsaturated C6-membered ring, and has been widely applied as vital building block in the synthesis of various chiral pharmaceuticals, agrochemicals and natural products, including immunosuppressant drug Tacrolimus (Kocieński et al., 1990), antitumor drug (+)-Phyllanthocin (Martin et al., 1989), cockroach attractant (−)-Periplanone-B (Kuwahara and Mori, 1990), neuraminidase inhibitor oseltamivir phosphate (Raghavan and Babu, 2011), and factor Xa inhibitor Edoxaban (Wang et al., 2017) etc. Especially, Edoxaban is a novel, selective, and orally active factor Xa inhibitor for the treatment of stroke and thromboembolic diseases. Optically active (*S*)-CHCA can be synthesized via several approaches: Diels-Alder reactions (Kocieński et al., 1990), resolution of the corresponding racemic acids employing chiral auxiliaries (Xu et al., 2013), and enantioselective hydrolysis of methyl 3-cyclohexene-1-carboxylate (CHCM) using microorganisms or isolated enzymes (Dou et al., 2020; Tanyeli and Turkut, 2004).

The critical problems in chemical synthesis are the lengthy reaction

* Corresponding author.
E-mail address: yni@jiangnan.edu.cn (Y. Ni).

https://doi.org/10.1016/j.biortech.2020.123984
Received 12 July 2020; Received in revised form 5 August 2020; Accepted 6 August 2020
Available online 10 August 2020
0960-8524/

steps, low yield and expensive chiral auxiliaries, resulting in low atomic economy. Biosynthesis could serve as an alternative method due to its relatively high efficiency, high enantioselectivity, and mild reaction conditions. However, few enzymes have been reported with desirable properties. Several commercial enzymes have been evaluated by Tanyeli *et al* in the preparation of (*S*)-CHCA from CHCM (Tanyeli and Turkut, 2004). Commercial esterases from porcine liver (PLE) and horse liver (HLE) were proved to be effective in kinetic resolution of 71 mM CHCM (10 $g{\cdot}L^{-1}$) with high enantioselectivity and conversion. However, the application of these animal-derived could be hampered by their high cost, low substrate loading, and interference by isozymes. Recently, a carboxylesterase BioH from *Escherichia coli* was reported as the first recombinant enzyme for the enantioselective hydrolysis of CHCM, giving ee_p of 32.3% and enantioselectivity (*E* value) of 2.1. Furthermore, through protein engineering by modulation of steric and aromatic interactions, a triple mutant Mu3 (L24A/W81A/L209A) was identified with increased ee_p of 70.9% and *E* value of 7.1, however, with compromised activity (Wu et al., 2019). The low enantioselectivity might be attributed to the highly symmetric structure of 3-cyclohexene group which is hard to be discriminated by enzymes. As a result, the efficient and enantioselective synthesis of Edoxaban precursors remains challenging.

In our previous endeavor, *Acinetobacter* sp. JNU9335 was isolated from soil samples, and exhibited high hydrolytic activity toward (*R*,*S*)-CHCM for the preparation of (*S*)-CHCM (Dou et al., 2020). Although JNU9335 could be used for the synthesis of Edoxaban precursor, the low contents of functional enzymes and excessive loading of microbial cells could result in high biocatalyst cost and compromised enantioselectivity as interfered by other intracellular enzymes. Moreover, high biocatalyst loading often leads to severe emulsification, complicated product recovery process, and low isolation yield. Therefore, high substrate loading (100 $g{\cdot}L^{-1}$) and high substrate to catalyst ratio (> 50) are difficult to achieve, which are important parameters for industrial manufacture (Luetz et al., 2008).

Considering the critical step in the resolution of CHCM is the hydrolysis of carboxylic ester bond, esterolytic enzymes play a key role in this process. Carboxylesterases (E.C. 3.1.1.1), a member of the esterolytic enzymes family, could catalyze both the cleavage and formation of carboxyl ester bonds (Bornscheuer, 2003). Carboxylesterases, also regarded as “true” esterases, are widely distributed in microorganism, plants and animals, and have high activity, broad substrate specificity, high regio- and enantio-selectivity (Yoon et al., 2003; Sungkeeree et al., 2018). Carboxylesterases are promising industrial biocatalysts (Schulze and Wubbolts, 1999), especially in the synthesis of chiral carboxylic acids, which are usually difficult to be synthesized by using other industrially relevant enzymes.

In this study, a genome shotgun library of *Acinetobacter* sp. JNU9335 was constructed to identify CHCM-hydrolyzing enzymes for the preparation of (*S*)-CHCM. A sensitive and reliable high-throughput screening method based on CHCA produced from hydrolysis of CHCM was established. A novel carboxylesterase, designated as *Ac*Est1, was identified with high efficiency in the enantioselective hydrolysis of *rac*-CHCM. The biochemical properties of purified *Ac*Est1 were characterized. The application of recombinant *Ac*Est1 in the synthesis of Edoxaban precursor was also investigated. This study indicates that *Ac*Est1 is a promising biocatalyst for the efficient biosynthesis of chiral carboxylic acids.

2. Materials and methods

2.1. Chemical, strains and plasmid

(*R*,*S*)-methyl 3-cyclohexene-1-carboxylate (*rac*-CHCM) and (*R*,*S*)-3-cyclohexene-1-carboxylate were bought from Shanghai Macklin Biochemical Co., Ltd. Three 3-cyclohexene-1-carboxylate esters with short-chain alcohol groups were prepared in laboratory and verified by nuclear magnetic resonance (NMR). *p*NP esters were purchased from Aladdin Co., Ltd. All other chemicals and reagents were of analytical grade and obtained from Sinopharm Co., Ltd. *Acinetobacter* sp. JNU9335 was screened from the soil and deposited at China General Microorganisms Collection and Management Center (CGMCC) under the accession number of CGMCC 17220. Plasmid pUC118 *Bam*H I/BAP vector was bought from Takara Co., Ltd.

2.2. High-throughput screening method

The high-throughput screening (HTS) was performed as previously described (Wang et al., 2012) with modification according to the characteristic of CHCA. The HTS reaction mixture is 200 μL and consisted of 10 μL bromothymol blue sodium solution (0.5 $mg{\cdot}mL^{-1}$, 5 mM pH 8.5 Tris-HCl), 10 μL phenol red solution (0.5 $mg{\cdot}mL^{-1}$, 5 mM pH 8.5 Tris-HCl), 60 μL $CaCl_2$ solution (100 mM, 5 mM pH 8.5 Tris-HCl), 80 μL dimethylformamide (DMF) and 40 μL different concentrations of CHCA solution (5% DMF) or CHCM (10 mM) reaction solution. The double indicator, calcium chloride solution and DMF were mixed together and added to each well. Then CHCM reaction solution was added and the color change was measured spectrophotometrically at 630 nm.

2.3. Identification of CHCM-hydrolyzing enzymes from shotgun library

Genomic DNA of strain JNU9335 was extracted from exponentially grown cells using a genomic DNA isolation kit. Genomic DNA was partially digested with *Sau3A* I. The DNA fragments with about 2.0–6.0 kb in length were recovered, and ligated into the *Bam*H I site (GATC) of commercial plasmid pUC118 *Bam*H I/BAP vector for overnight at 16 °C, and then transformed into *E. coli* DH5α to form the shotgun library of strain JNU9335.

The recombinants were grown on LB medium plate supplemented with 100 $\mu g{\cdot}mL^{-1}$ Ampicillin and 20 $\mu g{\cdot}mL^{-1}$ X-gal. The white colonies were picked up and incubated in a 96-deep-well microtitre plate containing 300 μL LB medium per well, and cultivated at 37 °C and 180 rpm for 12–16 h. An equivalent culture (100 μL) from each well was transferred into another 96-deep-well microtitre plate containing 500 μL LB medium per well. After cultivation at 37 °C and 180 rpm for 2–3 h, 0.2 mM IPTG was supplemented into each well and further induction at 25 °C and 180 rpm for 8 h. Then, recombinant cells were harvested by centrifugation at 10,000 × *g* and 4 °C for 20 min), followed by frozen at –80 °C for 12 h and lysed with lysozyme solution (0.75 $mg{\cdot}mL^{-1}$, 10 mM pH 8.5 Tris-HCl) at 37 °C for 1 h to form the crude extract of library of JNU9335. Furthermore, the library of strain JNU9335 was screened by high-throughput screening method described in 2.2.

The positive clones with obvious color changes in 96-well plates were selected and further cultivated in fresh LB liquid medium in flask for further evaluation with CHCM as testing substrate. The *ee* values of product (ee_p) were determined by HPLC (Infinity II; Agilent Technologies) equipped with a UV detector and a Chiral S-AY chromatography column (0.46 cm × 15 cm, 5 μm; Shanghai Chiralway Biotech Co., Ltd.), using mobile phase of n-hexane:isopropanol:trifluoroacetate = 99:1:0.02(v/v/v) at a flowrate of 0.7 $mL{\cdot}min^{-1}$, detection wavelength of 210 nm, column temperature of 25 °C, and injection volume of 10 μL. The retention times of (*R*)- and (*S*)-CHCA were 10.4 and 11.6 min, respectively. The *ee* values of the substrate (ee_s) were measured by Gas Chromatography equipped with an ASTEC chiraldex B-DM GC column (0.25 mm × 30 m). The injector and detector temperatures were both set at 280 °C, and a programmed temperature was adopted for column by keeping at 50 °C for 20 min, further increasing to 100 °C at 2 $°C{\cdot}min^{-1}$ and keeping for 10 min. The retention times of (*R*)- and (*S*)-CHCM were 47.9 min and 48.6 min respectively. The enantiomeric excess values of substrate (ee_s) and product (ee_p) were calculated using the following formula (Zhang et al., 2018b).

$$ee_s = \frac{[S1] - [R1]}{[S1] + [R1]} \times 100\%$$

$$ee_p = \frac{[R2] - [S2]}{[R2] + [S2]} \times 100\%$$

where [R1] and [S1] refer to the peak areas of (*R*)-CHCM and (*S*)-CHCM, [R2] and [S2] refer to the peak areas of (*R*)-CHCA and (*S*)-CHCA.

2.4. Bioinformatic analyses

Three positive clones were obtained with evident product peak. The plasmids were extracted, designated as pDZ01, pDZ02 and pDZ03, and sequenced. The open reading frames in these three plasmids were analyzed and predicted with ORF finder (https://www.ncbi.nlm.nih.gov/orffinder). The full-length gene coding for *Ac*Est1 was deposited at GenBank under accession No: MN984351. Alignment of *Ac*Est1 and homologous enzymes was conducted with ESPRIPT3.0 (Robert and Gouet, 2014). Phylogenetic analysis was performed by MEGA-X using the Neighbor-Joining method with 1000 replicates of bootstrapping analysis (Kumar et al., 2018).

2.5. Gene expression and purification of AcEst1

Based on the ORF analysis of pDZ01, pDZ02 and pDZ03, four potential putative esterases or α/β fold hydrolases were identified as *Ac*Est1, *Ac*Est2, *Ac*Est3 and *Ac*Est4. Subcloning of them were exemplified with *Ac*Est1. The *Ac*Est1 gene was amplified by PCR with pDZ01 as template and the following primers (Forward: gtgccgcgcggcagccatatgATGGGCGTGTTGAATCAAACTT, Reverse: gtggtggtggtggtgctcgagTTATTTGGCATTCTTATCCCAAAA). The PCR product was inserted into pET28a, linearized by double digestion with *Nde* I and *Xho* I, to generate the recombinant plasmid pET28-*Ac*Est1. Then, the resultant recombinant plasmid was transformed into *E. coli* BL21(DE3). After validation by sequencing, the positive transformant was inoculated into 100 mL fresh LB medium and cultivated until the OD_{600} reached 0.8. Then, IPTG (0.2 mM) was supplemented to induce the expression of *Ac*Est1 at 25 °C for 12 h. Furthermore, the cells were harvested by centrifugation at 10,000 × *g* and 4 °C for 20 min, washed with normal saline and re-suspended in 10 mL binding buffer (50 mM pH 7.4 NaH_2PO_4 and Na_2HPO_4, 20 mM imidazole, 500 mM NaCl). The cells were disrupted by ultrasonication (working 2 s and stopping 3 s for 10 min, 150 W), and the cell debris were removed by centrifugation at 4 °C and 10,000 × *g* for 20 min to obtain the crude enzyme. Then, the crude enzyme was filtered with 0.22 μm filters, loaded on a 1.0 mL Ni–NTA-Sefinose column (Sangon Biotech Co., Ltd), and eluted using elution buffer (50 mM pH 7.4 NaH_2PO_4 and Na_2HPO_4, 500 mM NaCl) with linear elevated imidazole concentrations from 20 mM to 500 mM. The purity and molecular weight of purified *Ac*Est1 were evaluated by SDS-PAGE analysis, and the concentration of purified *Ac*Est1 was determined using Nanodrop 2000 (Thermo Electron Co., Ltd).

2.6. Characterization of purified AcEst1

2.6.1. Activity assay

The general protocol for determination of the hydrolytic activity of *Ac*Est1 toward CHCM was as follows: 1 mM *rac*-CHCM (dissolved in acetonitrile, 5% v/v), PBS buffer (pH 7.0, 100 mM) and appropriate amount of *Ac*Est1 in total of 500 μL. Reaction was conducted at 30 °C and 180 rpm for 10 min, then terminated by addition of 1.0 M HCl. The sample was extracted with EtOAc, and the upper organic phase was isolated and dried over anhydrous Na_2SO_4, subjected to HPLC and GC analysis. The activity toward **S11** was spectrophotometrically assayed according to optical absorption changes of *p*-nitrophenol at 405 nm. A 200 μL reaction mixture, including 10 μL **S11** (0.5 mM), 10 μL enzyme solution and 180 μL PBS buffer (pH 7.0, 100 mM), was incubated at 30 °C. The OD_{405} of the reaction mixture was monitored for 3 min. One unit of activity (U) was defined as the amount of *Ac*Est1 required to catalyze the formation of 1 μmol of CHCA or *p*-nitrophenol per minute.

2.6.2. Effects of temperature and pH

Influence of pH on activity of *Ac*Est1 was evaluated at pH values ranging from 4.0 to 10.0, using sodium citrate buffer (pH 4.0–6.0, 100 mM), sodium phosphate buffer (pH 6.0–7.0, 100 mM), Tris-HCl buffer (pH 7.0–9.0, 100 mM) and glycine-NaOH buffer (pH 9.0–10.0, 100 mM). Effect of temperature on activity of *Ac*Est1 was measured by determining the relative activity toward **S11** at temperature ranges of 20–60 °C in PBS buffer (pH 7.0, 100 mM). The thermal stability of purified *Ac*Est1 was determined by examining the residual activity of preincubated enzyme solution at 30, 40 and 50 °C for indicated periods of time. All activity assay was carried out in triplicate.

2.6.3. Effect of metal ions and chemical agents

The effects of metal ions (Cu^{2+}, Al^{3+}, Ag^{+}, Mn^{2+}, Ca^{2+}, Ni^{2+}, Co^{2+}, Zn^{2+}, Fe^{2+}, and Mg^{2+}), organic solvents (methanol, ethanol, isopropanol, acetone, acetonitrile, tetrahydrofuran, DMSO, DMF) and surfactants (SDS, Tween-80 and Triton X-100) on the activity of *Ac*Est1 were explored in Tris-HCl buffer (pH 7.0, 100 mM) at 30 °C. Appropriate amount of purified *Ac*Est1 was incubated with various metal ions (1 mM), solvents (5%, v/v) and surfactants (0.1%) for indicated periods of time. Control experiment with addition of equal volume of Tris-HCl buffer at same incubation time was regarded as 100%. All activity assays were carried out in triplicate.

2.6.4. Kinetic parameters

Kinetic parameters were determined using the general activity assay protocol, except with different CHCM (1.0–20 mM) and **S11** (0.1–1.5 mM) concentrations were used. The kinetic parameters were calculated according to non-linear curve fitting with Michaelis–Menten equation.

2.6.5. Substrate specificity

*p*NP esters containing acyl chains with different length and structure (acetate, butyrate, caproate, caprylate, laurate, myristate, palmitate, trimethyl acetate, (+)-biotinate, Bis-*p*NP phosphate and CHCA) were used to determine the substrate specificity. Additionally, activity and enantioselectivity of *Ac*Est1 toward esters with various alcohol groups were determined, including CHCM, CHCE, CHCIP and CHCB. Appropriate amount of *Ac*Est1 was added to start the reaction until the conversion reached around 50%. The assays were carried out in standard conditions (100 mM PBS, pH 7.0, 30 °C). At different time intervals, samples were withdrawn and processed as above mentioned for chiral GC and HPLC analysis. All the measurements were performed in triplicate.

2.7. Kinetic resolution of rac-CHCM for the synthesis of (S)-CHCM

A reaction mixture including 200 mL Tris-HCl (pH 8.0, 200 mM), 16 mg dried cells of *Ac*Est1 (22 $U \cdot mg^{-1}$ cell), and 400 mmol (56.1 g) CHCM was magnetically stirred at 30 °C. Samples were taken at intervals and immediately analyzed for ee_s. The pH of reaction mixture was maintained at 8.0 by titration with Na_2CO_3 (1.0 M). After the ee_s value reached over than 99%, the reaction mixture was extracted with EtOAc under alkaline conditions. First, appropriate amount of 2.0 M NaOH was added to adjust the reaction mixture to pH 12.0. Then, 200 mL EtOAc was added to the reaction mixture and thoroughly extracted for three times. All the organic layers were combined, dried over anhydrous Na_2SO_4, and evaporated by vacuum distillation at 50 °C until a constant weight was observed. The isolated product was verified to be (*S*)-CHCM by NMR.

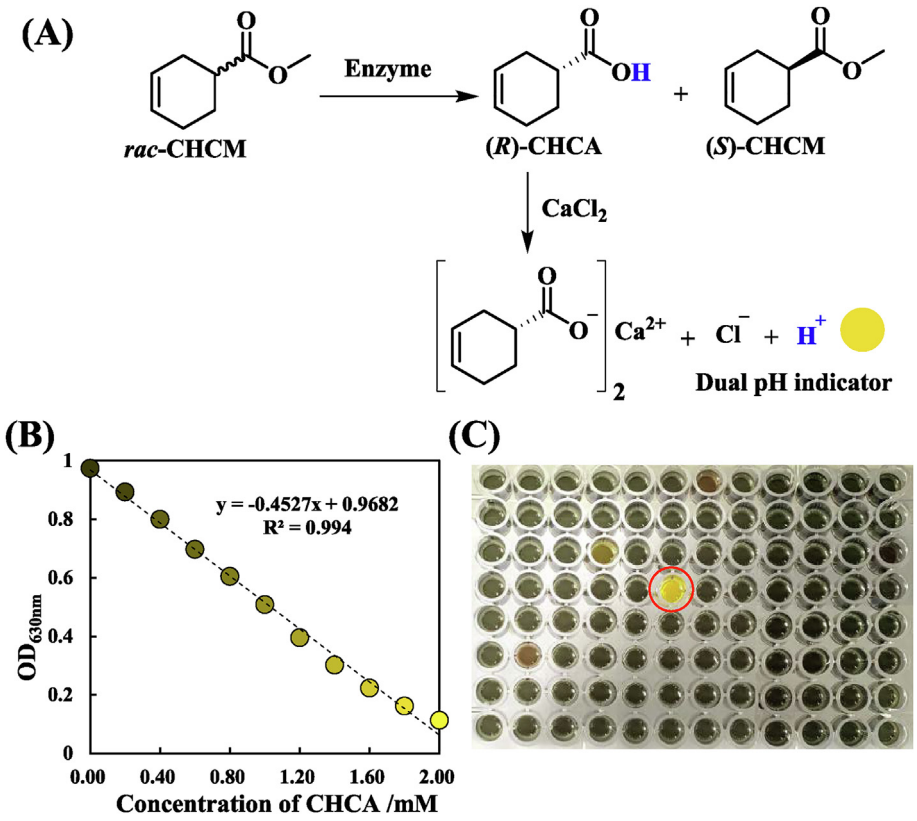

Fig. 1. Schematic overview of high-throughput screening method using dual pH indicators. (A) principle of this method, (B) calibration curve of CHCA, (C) result of the 96-well plate containing pDZ01 (indicated as red cycle). (For interpretation of the references to color in this figure legend, the reader is referred to the web version of this article.)

3. Results and discussion

3.1. Establishment of high-throughput screening method

To identify the CHCM-hydrolyzing enzymes from *Acinetobacter* sp. JNU9335, a quantifiable and high-throughput screening (HTS) method based on the production of CHCA was developed. The principle of this HTS method is that reaction between CHCA and $CaCl_2$ produces protons, which can be easily monitored by a pH indicator (Fig. 1A). To improve the sensitivity of this method, a dual pH indicator was adopted, including bromothymol blue sodium and phenol red with maximum absorbance peak at 630 nm (Wang et al., 2012). Compared with single pH indicator, it is more sensitive in determination of protons due to different color ranges of the two indicators (bromothymol blue, color changes from yellow to blue at pH range of 6.0–7.6; Phenol red, color changes from yellow to orange at pH range of 6.8–8.0). With the increase of protons, the color of double indicators changes from brownish green to yellow. To evaluate the feasibility of this HTS method, different concentrations of CHCA ranging from 0 to 2.0 mM were precipitated by calcium salt and mixed with the dual indicator. As shown in Fig. 1B, there is a linear correlation between OD_{630} of the reaction mixtures and the concentrations of CHCA, especially at lower concentrations (< 1.0 mM) of CHCA, indicating this HTS method is sensitive and effective in determination of enzyme activity. Further increase CHCA to higher than 2.0 mM resulted in higher amount of calcium salt complex and decrease in OD_{630}, which is hard to be monitored by a micro plate reader. However, the color at higher concentrations (bright yellow) of CHCA, indicating higher enzyme activity, was distinct from lower concentrations (brownish green) of CHCA and can be easily distinguished (Fig. 1B). Furthermore, CHCM was also evaluated and no color changes were observed, demonstrating the existence of CHCM had no interference effect on chromogenic reaction of CHCA.

3.2. Identification of AcEst1 from shotgun gene library of Acinetobacter sp. JNU9335

The whole-genome shotgun library of *Acinetobacter* sp. JNU9335 was developed by digestion of genomic DNA using *Sau3A* I. About 10,000 clones were picked and subjected to HTS. Positive transformants with distinct color change (OD_{630} < 0.2) were selected to further determine the activity and enantioselectivity toward CHCM (Fig. 1C). Three clones, designated as pDZ01, pDZ02 and pDZ03, showed apparent CHCA peaks according to HPLC analysis. The plasmids were sequenced with inserted DNA fragment of 3376 bp, 2900 bp and 3958 bp for pDZ01, pDZ02 and pDZ03 respectively. As analyzed by ORF finder, four putative hydrolytic enzymes were identified (Fig. 2A) and designated as *Ac*Est1 (1074 bp), *Ac*Est2 (870 bp), *Ac*Est3 (774 bp) and *Ac*Est4 (1014 bp). All the four putative hydrolytic enzymes were subcloned into pET28a and heterogenous expressed in soluble form in *E. coli* BL21(DE3). The specific activities toward *rac*-CHCM of *Ac*Est1–4 were 4.67, 0.05, 0.05 and 0.01 $U{\cdot}mg^{-1}$, respectively. And the ee_p values were 95% (*R*), 11% (*R*), 15% (*S*), and 73% (*R*) respectively at conversion of 10%. Considering the highest activity and enantioselectivity of *Ac*Est1, which is also similar to *Acinetobacter* sp. JNU9335 (Dou et al., 2020), *Ac*Est1 was selected as the target enzyme in further study.

Phylogenetic analysis was performed by sequence alignment of *Ac*Est1–4 and other lipolytic/esterolytic enzymes from families I to VIII. As shown in Fig. 2B, *Ac*Est1 located in the branch of family IV. Other known enzymes in family IV include carboxylesterases Est3K (Kim et al., 2015), EstDZ2 (Zarafeta et al., 2016), 7N9 (Borchert et al., 2017) etc. The amino acid sequences of carboxylesterases in family IV are similar to mammalian hormone-sensitive lipase (Østerlund, 2001), indicating a common evolutionary origin of bacterial and mammalian lipolytic enzymes (Rhee et al., 2005). Multiple sequence alignments indicate that *Ac*Est1 contains the highly conserved HGG motif involved in oxyanion hole formation, characteristic GDSAG, together with catalytic Ser201 along with an acidic Asp200 and a His325 constituting a highly conserved catalytic triad (Mohamed et al., 2013; Ramnath et al.,

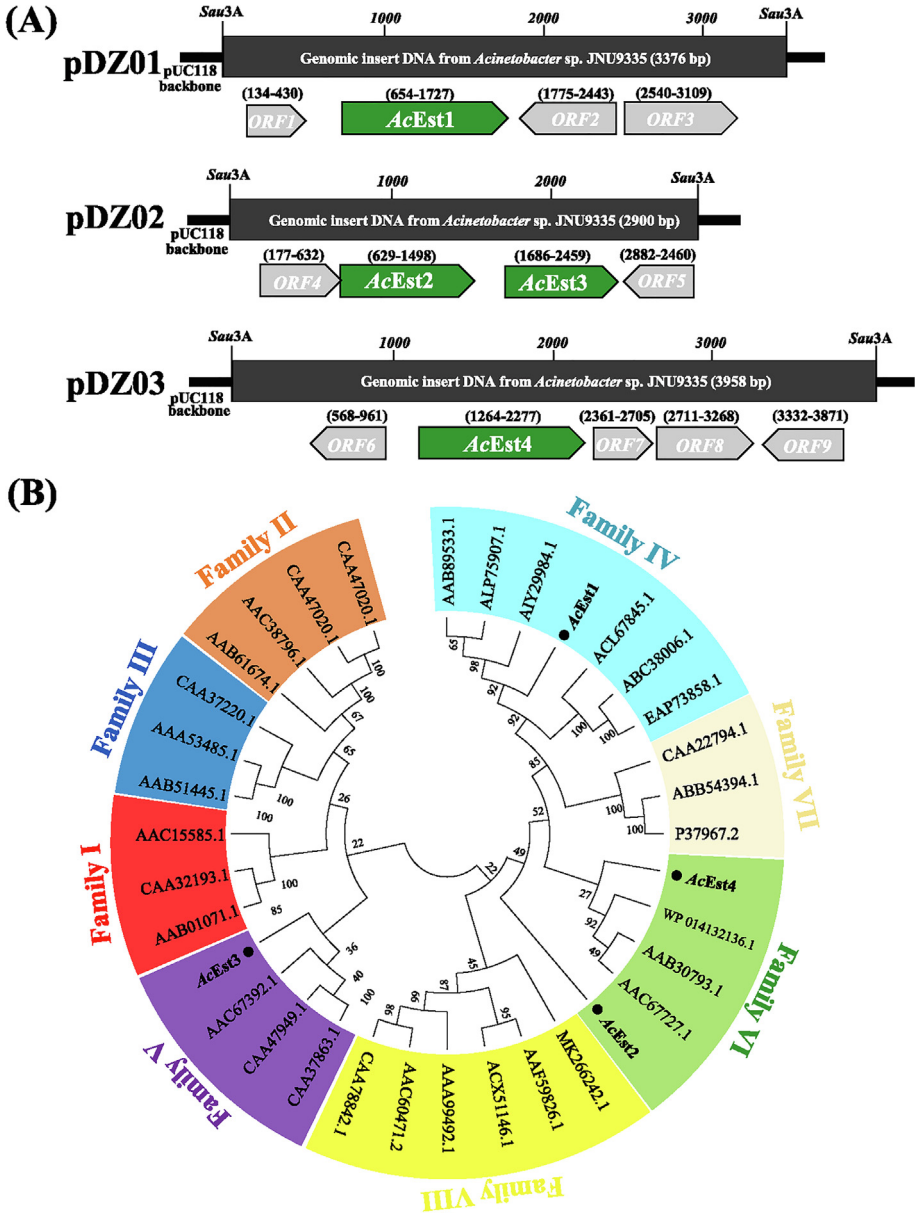

Fig. 2. (A) Schematic diagram of plasmids pDZ01–03 containing *Ac*Est1–4 encoding genes from *Acinetobacter* sp. JNU9335. The arrows with the nucleotide number in parentheses indicate the locations and directions of ORFs, with putative genes shaded in grey and *Ac*Est1–4 genes in green, ORFs < 300 bp were not shown. (B) Phylogenetic relationships of *Ac*Est1–4 and other known lipolytic/esterolytic enzymes. All protein sequences were retrieved from GenBank database. The phylogenetic tree was constructed by Neighbor-Joining method in MEGA-X 10.0 based on 1000 replicates. (For interpretation of the references to color in this figure legend, the reader is referred to the web version of this article.)

2017). *Ac*Est1 displays low identity with other reported carboxylesterases. The highest identity of 70.1% is found with carboxylesterase NlhH from *Acinetobacter* sp. KPC-SM-21. However, the functionality and properties of NlhH are unknown. Among the reported carboxylesterases, *Ac*Est1 displays 33.2% identity with carbolic ester hydrolase LipN from *Mycobacterium tuberculosis*, with probable role in xenobiotic degradation (Jadeja et al., 2016). The sequence identity between *Ac*Est1 and BioH (Wu et al., 2019) with CHCM hydrolytic activity is only 8.3%. Above results demonstrate that *Ac*Est1 is a novel carboxylesterase of family IV.

3.3. Characterization of AcEst1

To investigate the enzymatic properties of *Ac*Est1, recombinant *Ac*Est1 was purified to electrophoresis purity and migrated at around 40 kDa (Fig. 3A). The specific activity of purified *Ac*Est1 was 56 $U \cdot mg^{-1}$, indicating a purification fold of 12. The effects of temperature, pH, metal ions and additives on the activity and stability of purified *Ac*Est1 were examined using 4-nitrophenyl 3-cyclohexene-1-carboxylate (**S11**) as the substrate (Fig. 3).

The pH of reaction mixture might influence the activity of enzymes by affecting the conformations or protonation states of catalytic residues (Fersht and Alan, 1985). As illustrated in Fig. 3B, the highest activity of *Ac*Est1 was observed at pH 9.0. However, under alkalic conditions (pH > 8.0), **S11** is much more susceptible to spontaneous hydrolysis. No spontaneous hydrolysis of **S11** was observed in 100 mM Tris-HCl pH 8.0. Thus, pH 8.0 (Tris-HCl buffer) was regarded as the optimal pH for the subsequent characterization. It should be noted that at pHs lower than 7.0, the activity of *Ac*Est1 decreased significantly, such as only < 1% at pH 6.0, indicating the deleterious effect of acidic conditions on *Ac*Est1. Thus, the pH of the reaction mixture should be monitored in order to achieve efficient biotransformation at high substrate loading. The preferable performance of *Ac*Est1 in alkaline solutions is in line with other microbial esterases, such as esterases from *Bacillus aryabhattai* (8.5) (Zhang et al., 2019), *B. thermocloaceae* (8.0) (Yang et al., 2019) and *B. licheniformis* (8.0) (Zhang et al., 2018a).

The activity of *Ac*Est1 gradually increased from 20 °C to 40 °C and reached the maximum at 40 °C (Fig. 3C). However, further increase of temperature resulted in decreased activity of *Ac*Est1, which might be attributed to the destruction of its tertiary enzyme structure. Therefore,

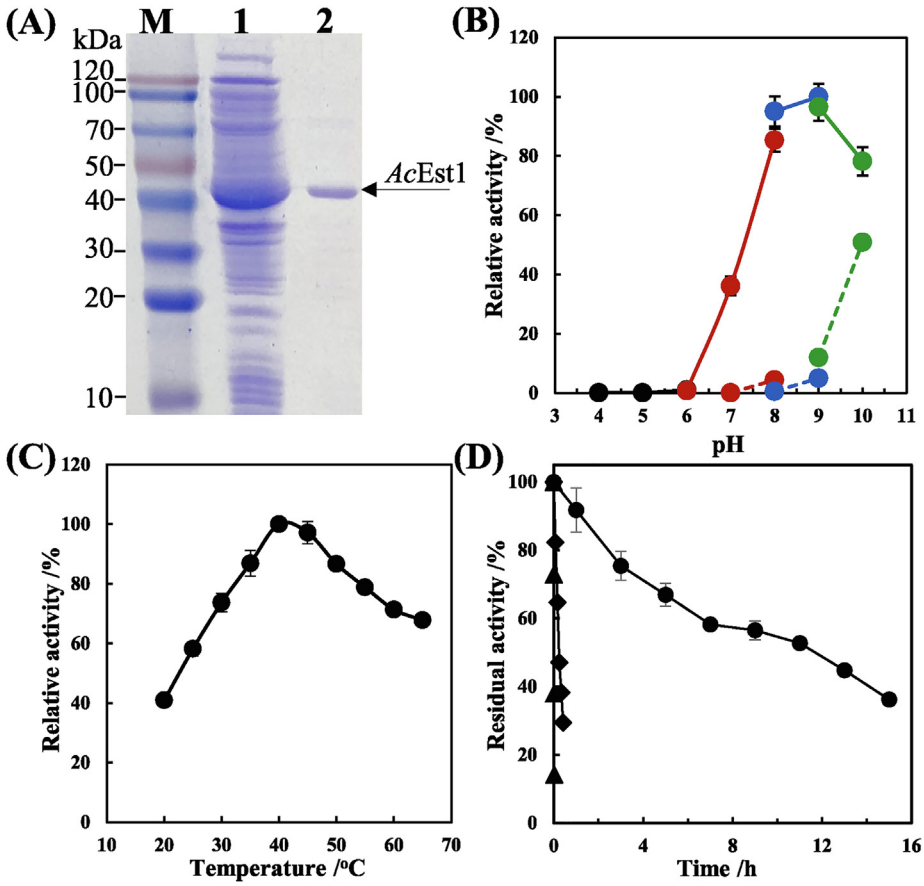

Fig. 3. Characterization of purified *Ac*Est1. (A) SDS-PAGE analysis of *Ac*Est1. M: protein marker, 1: crude enzyme solution, 2: purified *Ac*Est1; (B) pH: Solid line: activity toward **S11**, dashed line: spontaneous hydrolysis of **S11**, (●): sodium citrate buffer (pH 4.0–6.0), (●): sodium phosphate buffer (pH 6.0–7.0), (●): Tris–HCl buffer (pH 7.0–9.0), (●): Glycine-NaOH buffer (pH 9.0–10.0); (C) Temperature; (D) Thermostability: Circle: 30 °C, Diamond: 40 °C, Triangle: 50 °C.

the optimal temperature of *Ac*Est1 was determined to be 40 °C. The thermostability of *Ac*Est1 was also determined by measuring the residual activity after incubation at different temperatures. Despite of optimal temperature of 40 °C, *Ac*Est1 was not stable at over 40 °C. It was almost inactivated after incubation at 40 °C for 30 min and 50 °C for 5 min. At 30 °C for 3 h, the residual activity was about 75% of the initial activity (Fig. 3D). The half-life of *Ac*Est1 was calculated to be 9.7 h at 30 °C according to the Arrhenius deactivation equation. All above indicates that *Ac*Est1 is a mesophilic enzyme.

Influence of metal ions and chemical reagents on the activity of *Ac*Est1 was also explored (Table 1). No metal ions displayed significant promoting effect on the activity of *Ac*Est1. Cu^{2+}, Al^{3+} and Fe^{3+} inhibit its activity, similar to EstATII which was severely inhibited by Cu^{2+} (Mohamed et al., 2013). It is worth mentioning that the activity was deprived by about 50% by Ni^{2+}, suggesting *Ac*Est1 might have serine residues in the active center (Luo et al. 2015). In the presence of EDTA, 92.8% residual activity was retained, further proving that *Ac*Est1 does not depend on metal ions. Besides, SDS and CTAB completely inhibited the activity of *Ac*Est1. Inhibitory effect of SDS was also observed with serine hydrolases (Peng et al. 2011). Influence of several organic co-solvents was also investigated. Solvents, such as DMSO, DMF and ethanol, had little effect on the activity of *Ac*Est1, indicating its potential application in biocatalytic systems containing co-solvents.

Table 1
Effects of various metal ions and chemical reagents on the activity of *Ac*Est1.

Metal ion/ chemical reagent	Relative activity (%)	Chemical reagent	Relative activity (%)
Control	100.0 ± 2.3	CTAB	0.0
Cu^{2+}	5.0 ± 0.9	EDTA	92.8 ± 4.3
Al^{3+}	5.2 ± 0.3	Tween-80	95.5 ± 5.3
Ag^{+}	102.5 ± 1.1	Triton-X100	69.4 ± 6.0
Mn^{2+}	84.5 ± 2.4	Methanol	79.7 ± 1.9
Ca^{2+}	80.5 ± 1.0	Ethanol	95.8 ± 1.4
Ni^{2+}	46.4 ± 2.4	Isopropanol	100.0 ± 4.2
Co^{2+}	89.0 ± 0.7	Acetone	55.5 ± 5.6
Zn^{2+}	91.0 ± 3.7	Acetonitrile	22.3 ± 3.9
Fe^{3+}	5.1 ± 0.7	Tetrahydrofuran	17.2 ± 4.3
Mg^{2+}	89.0 ± 3.5	DMSO	89.3 ± 2.3
SDS	0.0	DMF	80.7 ± 0.6

Note: The concentration of metal ions and chemical reagents (CTAB, SDS, and EDTA) was 1 mM. Tween-80 and Triton-X100 were 1% (v/v), other chemical agents were 5% (v/v).

3.4. Substrate specificity of AcEst1

Substrate specificity of *Ac*Est1 was investigated using *p*-nitrophenyl esters with different acyl chains, including acetate (**S1**), butyrate (**S2**), caproate (**S3**), caprylate (**S4**), laurate (**S5**), myristate (**S6**), palmitate (**S7**), trimethyl acetate (**S8**), (+)-biotinate (**S9**), bis-pNP phosphate (**S10**) and CHCA ester (**S11**) (Fig. 4). Esters with different lengths of acyl groups can be used for rapid fingerprinting of lipolytic/esterolytic enzymes (Qian et al., 2011). As illustrated in Fig. 4, *Ac*Est1 showed typical non-lipolytic behavior, with a distinct preference toward esters with short chain fatty acids. A decrease in activity of *Ac*Est1 was observed along with the elongation of fatty acid chain, except for **S1**. *Ac*Est1 displayed the highest specific activity toward **S2** (51 $U \cdot mg^{-1}$). Only trace activity was determined with long-chain aliphatic esters such as **S5**, **S6** and **S7**. Branch-chain ester (**S8**) was an unfavorable substrate for *Ac*Est1, and the hydrolytic activity was merely 0.33 $U \cdot mg^{-1}$. Regarding **S9** and **S10** with large steric hindrance, *Ac*Est1 failed to exhibit any activity. Most importantly, **S11**, an analog of CHCM, could also be hydrolyzed by *Ac*Est1, with moderate activity of 12 $U \cdot mg^{-1}$. It has been reported that lipases prefer substrates with relatively long aliphatic chains (usually > 10 carbons) (Huang et al.,

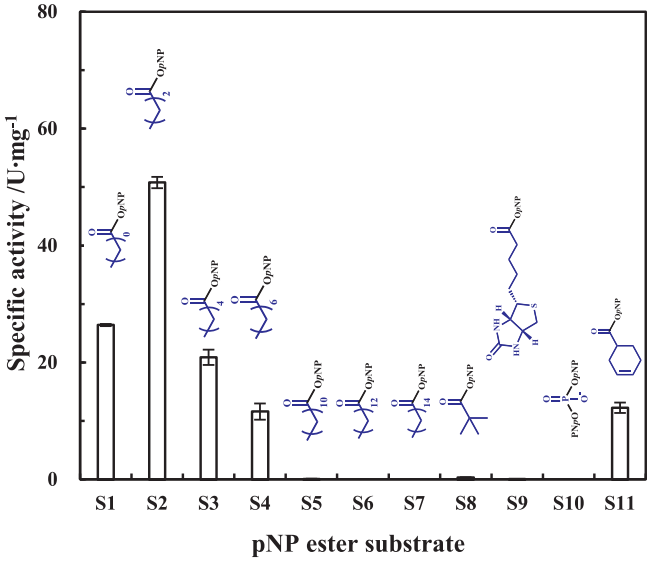

Fig. 4. Specific activity of *Ac*Est1 toward pNP esters with various aryl groups.

2020). As a result, *Ac*Est1 predominantly acts as an esterase rather than a lipase due to its preference toward short-chain esters such as *p*-nitrophenyl butyrate.

To further explore the influence of alcohol groups on activity and enantioselectivity of *Ac*Est1, four 3-cyclohexene-1-carboxylate esters including methyl (CHCM), ethyl (CHCE), isopropyl (CHCIP) and butyl (CHCB) were examined (Table 2). All of four esters could be hydrolyzed by *Ac*Est1. With the increase in size of alcohol groups, more time was required to reach around 50% conversion, indicating decreased activities of *Ac*Est1 toward esters with large alcohol groups. The decreased enantioselectivity, ee_s and ee_p, were also observed with the elongation of alcohol groups. For CHCM, the ee_s value is 73%, higher than 64% of CHCE, 66% of CHCIP and 19% of CHCB. Due to the highly symmetric and rotatable structure of 3-cyclohexene-1-carboxylate, few enzymes have been reported to discriminate two isomers of 3-cyclohexene-1-carboxylate esters with high activity and enantioselectivity. Among reported enzymes, recombinant carboxylesterase BioH exhibits 32% (*R*) toward CHCM (Wu et al., 2019), much lower than that of *Ac*Est1. Considering the high activity and enantioselectivity of *Ac*Est1 toward CHCM, biocatalytic preparation of (*S*)-CHCM was further investigated.

Table 2
Biocatalytic conversion of 3-cyclohexene-1-carboxylate esters by *Ac*Est1.

Substrate	Structural	ee_s (%)	ee_p (%)	Conversion (%)	Time (h)
CHCM		73	71	49	1
CHCE	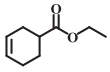	64	56	47	1
CHCIP	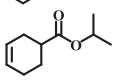	66	59	47	2
CHCB	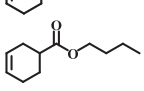	19	18	49	4

Note: The 10 mL reaction system consisted of *Ac*Est1 (1 mg) and 3-cyclohexene-1-carboxylate ester (final concentration of 50 mM) in sodium phosphate buffer (200 mM, pH 8.0) at 30 °C. CHCM: Methyl 3-cyclohexene-1-carboxylate, CHCE: Ethyl 3-cyclohexene-1-carboxylate, CHCIP: Isopropyl 3-cyclohexene-1-carboxylate, CHCB: Butyl 3-cyclohexene-1-carboxylate.

Table 3
Kinetic parameters of *Ac*Est1 toward **S11** and CHCM.

Substrate	K_M (mM)	V_{max} (μmol·min^{-1}·mg^{-1})	k_{cat} (s^{-1})	k_{cat}/K_M (s^{-1}·mM^{-1})
S11	0.63 ± 0.05	22.9 ± 0.7	15.3 ± 0.5	24.3 ± 0.8
CHCM	15.66 ± 5.68	1730 ± 44	1153 ± 29	73.6 ± 1.9

3.5. Kinetic parameters of AcEst1

The K_M values of *Ac*Est1 toward **S11** and CHCM were 0.63 and 15.66 mM respectively (Table 3). *Ac*Est1 exhibits higher affinity toward **S11** than CHCM. The V_{max} and k_{cat} values toward **S11** and CHCM of *Ac*Est1 were 22.9 μmol·min^{-1}·mg^{-1} and 15.3 s^{-1}, 1730 μmol·min^{-1}·mg^{-1} and 1153 s^{-1}, indicating *Ac*Est1 is highly efficient in the hydrolysis of 3-cyclohexene-1-carboxylate esters especially CHCM. The k_{cat}/K_M values toward **S11** and CHCM were calculated to be 24.3 and 73.6 s^{-1}·mM^{-1}, respectively. It is worth noting that no substrate inhibition was observed with CHCM and the catalytic efficiency of *Ac*Est1 is extremely high at high substrate loading. From a practical perspective, high catalytic activity at high substrate concentrations is one of the prerequisites of a promising biocatalyst. Consequently, *Ac*Est1 is a highly efficient biocatalyst with potential application in hydrolysis of 3-cyclohexene-1-carboxylate esters.

3.6. Enantioselective synthesis of (S)-CHCM catalyzed by AcEst1

High substrate loading is essential for the practical application of a biocatalytic process (Luetz et al., 2008). Application potential of recombinant *Ac*Est1 in the kinetic resolution of *rac*-CHCM at different loadings were explored for the biosynthesis of chiral (*S*)-CHCM. At 500 mM *rac*-CHCM (70 g·L^{-1}), 176 mM (*S*)-CHCM was obtained with > 99% ee_s using merely 0.02 g·L^{-1} *Ac*Est1 in 8 h (Fig. 5). The substrate to catalyst ratio (S/C) and space-time yield were calculated to be 3500 g·g^{-1} and 74 g·L^{-1}·d^{-1}. At increased substrate concentration of 1.0 M and the same S/C of 3500 g·g^{-1}, only 9 h was required to achieve about 360 mM (*S*)-CHCM in > 99% ee_s. The space-time yield at 1.0 M was calculated to be 140 g·L^{-1}·d^{-1}, almost 2-fold of that at 0.5 M *rac*-CHCM. The stable catalytic performance of *Ac*Est1 encouraged us to further elevate the substrate concentration to 2.0 M (280 g·L^{-1}). As

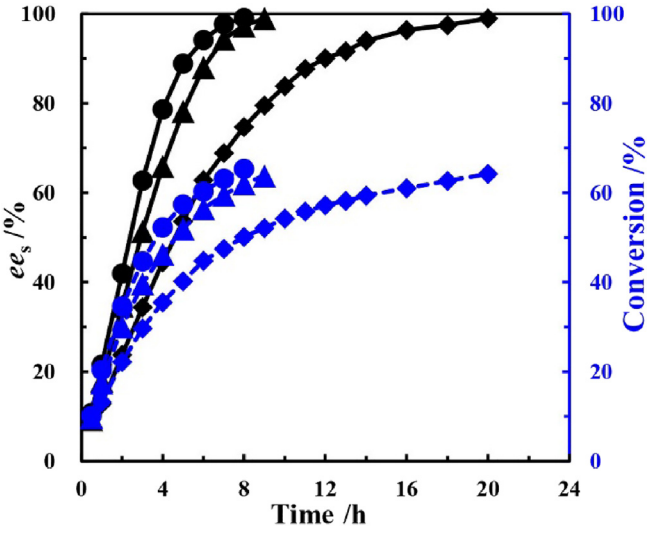

Fig. 5. Time course of kinetic resolution of *rac*-CHCM catalyzed by *Ac*Est1 at different substrate loadings. Circle: 500 mM (70 g·L^{-1}), triangle: 1.0 M (140 g·L^{-1}), diamond: 2.0 M (280 g·L^{-1}); black solid line: ee_s, blue dotted line: substrate conversion ratio. (For interpretation of the references to color in this figure legend, the reader is referred to the web version of this article.)

illustrated in Fig. 5, the ee_s gradually increased to > 99% at the end of 20 h. About 715 mM (*S*)-CHCM was obtained with a space-time yield of 121 $g{\cdot}L^{-1}{\cdot}d^{-1}$. Compared with 500 mM and 1.0 M, much longer reaction time is required which might be attributed to the mass-transfer limitation at 2.0 M *rac*-CHCM. It should be noted that there is no sacrifice in enantioselectivity of *Ac*Est1 even at 2.0 M substrate loading. A high as 2.0 M *rac*-CHCM could be enantioselectively hydrolyzed at S/C of 3500 $g{\cdot}g^{-1}$ by *Ac*Est1 within 20 h. Based on typical features of a "good" biocatalyst for an industrial bioprocess, including substrate loading ≥100 $g{\cdot}L^{-1}$, reaction time ≤24 h, *ee* ≥ 99% and biocatalyst loading ≤5 $g{\cdot}L^{-1}$ etc (Luetz et al., 2008), *Ac*Est1 is a promising biocatalyst with substrate loading of 280 $g{\cdot}L^{-1}$, reaction time of 20 h, ee_s of > 99%, and biocatalyst loading of merely 0.08 $g{\cdot}L^{-1}$. These results demonstrate that *Ac*Est1 is a robust biocatalyst for the enantioselective synthesis of Edoxaban precursor.

Performance of *Ac*Est1 in the enantioselective hydrolysis of *rac*-CHCM was compared with other reported commercial and recombinant enzymes. Commercial enzymes, PLE, HLE and PPL, were capable of resolution of *rac*-CHCM with relatively high enantioselectivity and space-time yields of 8.6–18.0 $g{\cdot}L^{-1}{\cdot}d^{-1}$ at S/C of 50 $g{\cdot}g^{-1}$. Carboxylesterase BioH from *E. coli* was the first recombinant enzyme with hydrolytic activity toward *rac*-CHCM, however, with 11% ee_s and 32% ee_p. Protein engineering of BioH was conducted and a triple mutant $BioH_{Mu3}$ (L24A/W81A/L209A) was obtained with 71% ee_p and compromised activity. At 40 mM *rac*-CHCM, the S/C decreased from 47 to 2 $g{\cdot}g^{-1}$ compared with wild type BioH. *Ac*Est1 exhibited stable performance in the enantioselective resolution of as high as 2.0 M *rac*-CHCM, with S/C of 3500 $g{\cdot}g^{-1}$, > 99% ee_s and a space–time yield of 121 $g{\cdot}L^{-1}{\cdot}d^{-1}$. The S/C of *Ac*Est1 is about 70-fold of commercial enzymes. To the best of the knowledge, *Ac*Est1 displays the highest catalytic performance. Presumably, significantly higher space-time yield could be easily achieved at enhanced biocatalyst loading. At biocatalyst loading of 5.0 $g{\cdot}L^{-1}$, the reaction time could be decrease from 20 h to < 30 min, and the productivity could be expected to reach *cal.* 4840 $g{\cdot}L^{-1}{\cdot}d^{-1}$ at 280 $g{\cdot}L^{-1}$ *rac*-CHCM, ascribing to the stable catalytic performance of recombinant *Ac*Est1. Consequently, this newly identified *Ac*Est1 is advantageous over previously reported enzymes in the kinetic resolution of CHCM. The structure and molecular mechanism for the high enantioselectivity and activity of *Ac*Est1, as well as recycling of *R*-enantiomer product are carrying out, which will provide guidance for scale-up biocatalytic synthesis of chiral Edoxaban precursor.

4. Conclusions

In this study, a new carboxylesterase *Ac*Est1 was identified by high-throughput screening of shotgun library of *Acinetobacter* sp. JNU9335. *Ac*Est1 displays low sequence identity with other known carboxylesterases. Recombinant *Ac*Est1 exhibited remarkable catalytic efficiency toward methyl 3-cyclohexene-1-carboxylate with k_{cat} of 1153 s^{-1}. In the biosynthesis of (*S*)-CHCM, enantioselectivity of > 99% ee_s was achieved at high substrate loading of 280 $g{\cdot}L^{-1}$, with an extraordinary substrate to catalyst ratio of 3500 $g{\cdot}g^{-1}$, demonstrating that *Ac*Est1 is promising biocatalyst for the large-scale preparation of (*S*)-CHCM, a key chiral precursor of Edoxaban.

CRediT authorship contribution statement

Zhe Dou: Investigation, Data curation, Writing - original draft, Validation. **Guochao Xu:** Methodology, Validation, Writing - review & editing. **Ye Ni:** Conceptualization, Supervision, Funding acquisition, Writing - review & editing.

Declaration of Competing Interest

The authors declare that they have no known competing financial interests or personal relationships that could have appeared to influence the work reported in this paper.

Acknowledgements

We are grateful to National Key Research and Development Program of China (2018YFA0901700), National Natural Science Foundation of China (21776112), Postgraduates Research & Practice Innovation Program of Jiangsu Province (KYCX20_1808), and National First-Class Discipline Program of Light Industry Technology and Engineering (LITE2018-07) for the financial support of this research.

Appendix A. Supplementary data

Supplementary data to this article can be found online at https://doi.org/10.1016/j.biortech.2020.123984.

References

Borchert, E., Selvin, J., Kiran, S.G., Jackson, S.A., O'Gara, F., Dobson, A.D.W., 2017. A novel cold active esterase from a deep sea sponge *Stelletta normani* metagenomic library. Front. Mar. Sci. 4, 287. https://doi.org/10.3389/fmars.2017.00287.

Bornscheuer, U.T., 2003. Microbial carboxyl esterases: Classification, properties and application in biocatalysis. FEMS Microbiol. Rev. 26, 73–81. https://doi.org/10.1111/j.1574-6976.2002.tb00599.x.

Dou, Z., Xu, G.C., Ni, Y., 2020. Efficient microbial resolution of racemic methyl 3-cyclohexene-1-carboxylate as chiral precursor of Edoxaban by newly identified *Acinetobacter* sp. JNU9335. Enzyme Microb. Technol. 139, 109580. https://doi.org/10.1016/j.enzmictec.2020.109580.

Fersht, Alan, 1985. Enzyme Structure and Mechanism, second ed. W.H Freeman and Company.

Huang, L., Meng, D., Tian, Q., Yang, S., Deng, H., Guan, Z., Cai, Y., Liao, X., 2020. Characterization of a novel carboxylesterase from *Bacillus velezensis* SYBC H47 and its application in degradation of phthalate esters. J. Biosci. Bioeng. 129, 88–594. https://doi.org/10.1016/j.jbiosc.2019.11.002.

Jadeja, D., Dogra, N., Arya, S., Singh, G., Singh, G., Kaur, J., 2016. Characterization of LipN (Rv2970c) of *Mycobacterium tuberculosis* H37Rv and its probable role in xenobiotic degradation. J. Cell Biochem. 117, 390–401. https://doi.org/10.1002/jcb.25285.

Kim, H.J., Jeong, Y.S., Jung, W.K., Kim, S.K., Lee, H.W., Kahng, H.Y., Kim, J., Kim, H., 2015. Characterization of novel family IV esterase and family I.3 lipase from an oil-polluted mud flat metagenome. Mol. Biotechnol. 57, 781–792. https://doi.org/10.1007/s12033-015-9871-4.

Kocieński, P., Stocks, M., Donald, D., Perry, M., 1990. A synthesis of the C24–C34 segment of FK 506. Synlett. 1, 38–39. https://doi.org/10.1055/s-1990-20978.

Kumar, S., Stecher, G., Li, M., Knyaz, C., Tamura, K., 2018. MEGA X: Molecular evolutionary genetics analysis across computing platforms. Mol. Biol. Evol. 35, 1547–1549. https://doi.org/10.1093/molbev/msy096.

Kuwahara, S., Mori, K., 1990. Synthesis of (–)-periplanone-B a sex pheromone component of the American cockroach (*periplaneta americana*). Tetrahedron. 46, 8075–8082. https://doi.org/10.1016/S0040-4020(01)81464-2.

Luetz, S., Giver, L., Lalonde, J., 2008. Engineered enzymes for chemical production. Biotechnol. Bioeng. 101, 647–653. https://doi.org/10.1002/bit.22077.

Luo, Z.H., Ding, J.F., Xu, W., Zheng, T.L., Zhong, T.H., 2015. Purification and characterization of an intracellular esterase from a marine *Fusarium* fungal species showing phthalate diesterase activity. Int. Biodeterior. Biodegrad. 97, 7–12. https://doi.org/10.1016/j.ibiod.2014.10.006.

Martin, S.F., Dappen, M.S., Dupré, B., Murphy, C.J., Colapret, J.A., 1989. Application of nitrile oxide cycloadditions to a convergent, asymmetric synthesis of (+)-phyllanthocin. J. Org. Chem. 54, 2209–2216. https://doi.org/10.1021/jo00270a035.

Mohamed, Y.M., Ghazy, M.A., Sayed, A., Ouf, A., El-Dorry, H., Siam, R., 2013. Isolation and characterization of a heavy metal-resistant, thermophilic esterase from a Red Sea brine pool. Sci. Rep. 3, 3358. https://doi.org/10.1038/srep03358.

Østerlund, T., 2001. Structure-function relationships of hormone-sensitive lipase. Eur. J. Biochem. 268, 1899–1907. https://doi.org/10.1046/j.1432-1327.2001.02097.x.

Peng, Q., Zhang, X., Shang, M., Wang, X., Wang, G., Li, B., Guan, G., Li, Y., Wang, Y., 2011. A novel esterase gene cloned from a metagenomic library from neritic sediments of the South China Sea. Microb. Cell Fact. 10, 95. https://doi.org/10.1186/1475-2859-10-95.

Qian, L., Liu, J.Y., Liu, J.Y., Yu, H.L., Li, C.X., Xu, J.H., 2011. Fingerprint lipolytic enzymes with chromogenic *p*-nitrophenyl esters of structurally diverse carboxylic acids. J. Mol. Catal. B-Enzym. 73, 22–26. https://doi.org/10.1016/j.molcatb.2011.07.010.

Raghavan, S., Babu, V.S., 2011. Enantioselective synthesis of oseltamivir phosphate. Tetrahedron. 67, 2044–2050. https://doi.org/10.1016/j.tet.2011.01.064.

Ramnath, L., Sithole, B., Govinden, R., 2017. Classification of lipolytic enzymes and their biotechnological applications in the pulping industry. Can. J. Microbiol. 63, 179–192.

https://doi.org/10.1139/cjm-2016-0447.
Rhee, J.K., Ahn, D.G., Kim, Y.G., Oh, J.W., 2005. New thermophilic and thermostable esterase with sequence similarity to the hormone-sensitive lipase family, cloned from a metagenomic library. Appl. Environ. Microbiol. 71, 817–825. https://doi.org/10.1128/AEM.71.2.817-825.2005.
Robert, X., Gouet, P., 2014. Deciphering key features in protein structures with the new ENDscript server. Nucl. Acids Res. 42, W320–W324. https://doi.org/10.1093/nar/gku315.
Schulze, B., Wubbolts, M.G., 1999. Biocatalysis for industrial production of fine chemicals. Curr. Opin. Biotechnol. 10, 609–615. https://doi.org/10.1016/S0958-1669(99)00042-7.
Sungkeeree, P., Toewiwat, N., Whangsuk, W., Ploypradith, P., Mongkolsuk, S., Loprasert, S., 2018. The esterase B from *Sphingobium* sp. SM42 has the new de-arenethiolase activity against cephalosporin antibiotics. Biochem. Biophys. Res. Commun. 506, 231–236. https://doi.org/10.1016/j.bbrc.2018.10.078.
Tanyeli, C., Turkut, E., 2004. Enzyme catalyzed reverse enantiomeric separation of methyl (±)-3-cyclohexene-1-carboxylate. Tetrahedron Asymmetry. 15, 2057–2060. https://doi.org/10.1016/j.tetasy.2004.05.034.
Wang, D., Wang, J., Wang, B., Yu, H.W., 2012. A new and efficient colorimetric high-throughput screening method for triacylglycerol lipase directed evolution. J. Mol. Catal. B-Enzym. 82, 18–23. https://doi.org/10.1016/j.molcatb.2012.05.021.
Wang, X., Ma, M.L., Reddy, A.G.K., Hu, W.H., 2017. An efficient stereoselective synthesis of six stereoisomers of 3, 4-diaminocyclohexane carboxamide as key intermediates for the synthesis of factor Xa inhibitors. Tetrahedron. 73, 1381–1388. https://doi.org/10.1016/j.tet.2017.01.021.
Wu, X.F., Yang, S.L., Yu, H.W., Ye, L.D., Su, B.M., Shao, Z.H., 2019. Improved enantioselectivity of *E. coli* BioH in kinetic resolution of methyl (*S*)-3-cyclohexene-1-carboxylate by combinatorial modulation of steric and aromatic interactions. Biosci. Biotechnol. Biochem. 83, 1263–1269. https://doi.org/10.1080/09168451.2019.1597620.
Xu, C.X., Shi, Y., Zhang, S.Y., Liu, R., Xia, C., Wei, H.Q., Li, W.L., 2013. Chiral resolution of cyclohex-3-ene-1-carboxylic acid. Drugs Clinic. 28, 126–128.
Yang, Y., Ghatge, S., Hur, H.G., 2019. Characterization of a novel thermostable carboxylesterase from thermoalkaliphilic bacterium *Bacillus thermocloaceae*. Biosci. Biotechnol. Biochem. 83, 882–891. https://doi.org/10.1080/09168451.2019.1574555.
Yoon, K.J.P., Krull, E.J., Morton, C.L., Bornmann, W.G., Lee, R.E., Potter, P.M., Danks, M.K., 2003. Activation of a camptothecin prodrug by specific carboxylesterases as predicted by quantitative structure-activity relationship and molecular docking studies. Mol. Cancer Ther. 2, 1171–1181 http://mct.aacrjournals.org/content/2/11/1171.
Zarafeta, D., Moschidi, D., Ladoukakis, E., Gavrilov, S., Chrysina, E.D., Chatziioannou, A., Kublanov, I., Skretas, G., Kolisis, F.N., 2016. Metagenomic mining for the thermostable esterolytic enzymes uncovers a new family of bacterial esterases. Sci. Rep. 6, 38886. https://doi.org/10.1038/srep38886.
Zhang, W., Xu, H., Wu, Y., Zeng, J., Guo, Z., Wang, L., Shen, C., Qiao, D., Cao, Y., 2018a. A new cold-adapted, alkali-stable and highly salt-tolerant esterase from *Bacillus licheniformis*. Int. J. Biol. Macromol. 111, 1183–1193. https://doi.org/10.1016/j.ijbiomac.2018.01.152.
Zhang, Y., Cheng, F., Yan, H., Zheng, J., Wang, Z., 2018b. The enzymatic resolution of 1-(4-chlorophenyl) ethylamine by Novozym 435 to prepare a novel triazolopyrimidine herbicide. Chirality. 30, 1225–1232. https://doi.org/10.1002/chir.23016.
Zhang, Y.J., Chen, C.S., Liu, H.T., Chen, J.L., Xia, Y., Wu, S.J., 2019. Purification, identification and characterization of an esterase with high enantioselectivity to *(S)*-ethyl indoline-2-carboxylate. Biotechnol. Lett. 41, 1223–1232. https://doi.org/10.1007/s10529-019-02727-w.